40 Gb/s optical subassembly module for a multi-channel bidirectional optical link

Jamshid Sangirov,[1,*] Gwan-Chong Joo,[2] Jae-Shik Choi,[2] Do-Hoon Kim,[2] Byueng-Su Yoo,[3] Ikechi Augustine Ukaegbu,[1] Nguyen T. H. Nga,[1] Jong-Hun Kim,[1] Tae-Woo Lee,[1] Mu Hee Cho,[1] and Hyo-Hoon Park[1]

[1]*Photonic Computer Systems Laboratory, Korea Advanced Institute of Science and Technology (KAIST), 291 Daehak-ro, Yuseong-gu, Daejeon 305-701, South Korea*
[2]*Hantech Co. Ltd., 372 Jung-Ri, Dongtan-Myeon, Hwaseong-Si, Gyeonggi-Do, 445-813, South Korea*
[3]*RayCan Co. Ltd., 138 Gajeong-dong, Yuseong-gu, Daejeon, 305-350, South Korea*
[*]*jamshid@kaist.ac.kr*

Abstract: A 40 Gb/s bidirectional optical link using four-channel optical subassembly (OSA) modules and two different wavelengths for the up- and down-link is demonstrated. Widely separated wavelengths of 850 nm and 1060 nm are used to reduce the optical crosstalk between the up- and down-link signals. Due to the integration capabilities of silicon, the OSA is implemented, all based on silicon: V-grooved silicon substrates to embed fibers and silicon optical benches (SiOBs) to mount optical components. The SiOBs are separately prepared for array chips of photodiodes (PDs), vertical-cavity surface-emitting lasers (VCSELs), and monitoring PDs, which are serially configured on an optical fiber array for direct coupling to the transmission fibers. The separation of the up- and down-link wavelengths is implemented using a wavelength-filtering 45° mirror which is formed in the fiber under the VCSEL. To guide the light signal to the PD another 45° mirror is formed at the end of the fiber. The fabricated bidirectional OSA module shows good performances with a clear eye-diagram and a BER of less than 10^{-12} at a data rate of 10 Gb/s for each of the channels with input powers of −8 dBm and −6.5 dBm for the up-link and the down-link, respectively. The measured inter-channel crosstalk of the bidirectional 40 Gb/s optical link is about −22.6 dB, while the full-duplex operation mode demonstrates negligible crosstalk between the up- and down-link.

OCIS codes: (200.4650) Optical interconnects; (060.2360) Fiber optics links and subsystems; (080.4035) Mirror system design; (130.7408) Wavelength filtering devices; (230.0230) Optical devices.

References and links

1. C. L. Schow, F. E. Doany, A. V. Rylyakov, B. G. Lee, C. V. Jahnes, Y. H. Kwark, C. W. Baks, D. M. Kuchta, and J. A. Kash, "A 24-channel, 300 Gb/s, 8.2 pJ/bit, full-duplex fiber-coupled optical transceiver module based on a single "holey" CMOS IC," J. Lightwave Technol. **29**(4), 542–553 (2011).
2. J.-Y. Park, H.-S. Lee, S.-S. Lee, and Y.-S. Son, "Passively aligned transmit optical subassembly module based on a WDM incorporating VCSELs," IEEE Photon. Technol. Lett. **22**(24), 1790–1792 (2010).
3. J. Sangirov, I. A. Ukaegbu, T.-W. Lee, M.-H. Cho, and H.-H. Park, "Signal synchronization using a flicker reduction and denoising algorithm for video-signal optical interconnect," ETRI Journal **34**(1), 122–125 (2012).
4. J. D. Ingham, R. V. Penty, and I. H. White, "Bidirectional multimode-fiber communication links using dual-purpose vertical-cavity devices," J. Lightwave Technol. **24**(3), 1283–1294 (2006).
5. N. T. H. Nguyen, J. Sangirov, D.-M. Im, M. H. Cho, T.-W. Lee, and H.-H. Park, "Bidirectional optical transceiver integrated with an envelope detector for automatically controlling the direction of transmission," Proc. ECTC, 2098–2100 (2009).
6. G.-C. Joo, S.-H. Lee, K.-S. Park, J.-S. Choi, N. Hwang, and M.-K. Song, "A novel bidirectional optical coupling module for subscribers," IEEE Trans. Adv. Packag. **23**(4), 681–685 (2000).
7. Y. S. Heo, H.-J. Park, H. S. Kang, and K.-S. Lim, "1/10 Gb/s single transistor-outline-CAN bidirectional optical subassembly for a passive optical network," Opt. Eng. Lett. **52**(1), 010501 (2013).

#200040 - $15.00 USD Received 23 Oct 2013; revised 7 Dec 2013; accepted 15 Dec 2013; published 17 Jan 2014

8. B. S. Rho, H. S. Cho, J.-Y. Eo, S.-K. Kang, H.-H. Park, Y. W. Kim, Y. S. Joe, and D. J. Yang, "New architecture of optical interconnection using 45°-ended connection rods in waveguide-embedded printed circuit boards," Proc. SPIE **4997**, 71–78 (2003).
9. Y. Nekado and M. Iwase, "1.3-μm range vertical-cavity surface-emitting laser (VCSEL) module," Furukawa Review **27**, 72–78 (2005).
10. K.-S. Lim, J. J. Lee, S. Lee, S. Yoon, C. H. Yu, I.-B. Sohn, and H. S. Kang, "A novel low-cost fiber in-line-type bidirectional optical subassembly," IEEE Photon. Technol. Lett. **19**(16), 1233–1235 (2007).
11. D. Paladino, A. Iadicicco, S. Campopiano, and A. Cusano, "Not-lithographic fabrication of micro-structured fiber Bragg gratings evanescent wave sensors," Opt. Express **17**(2), 1042–1054 (2009).
12. J. A. Lott, V. A. Shchukin, N. N. Ledentsova, A. Stintz, F. Hopfer, A. Mutig, G. Fiol, D. Bimberg, S. A. Blokhin, L. Y. Karachinsky, I. I. Novikov, M. V. Maximov, N. D. Zakharov, and P. Werner, "20 Gbit/s error free transmission with ~850 nm GaAs-based vertical cavity surface emitting lasers (VCSELs) containing InAs-GaAs submonolayer quantum dot insertions," Proc. SPIE **7211**(14), 1–12 (2009).
13. A. Mutig, P. Mosera, J. A. Lott, P. Wolf, W. Hofmann, N. N. Ledentsov, and D. Bimberg, "High-speed 850 and 980 nm VCSELs for high-performance computing applications," Proc. SPIE **7338**(19), 1–7 (2011).
14. M. Hostut, A. Kilic, S. Sakiroglu, Y. Ergun, and I. Sokmen, "Voltage tunable dual-band quantum-well infrared photodetector for third-generation thermal imaging," IEEE Photon. Technol. Lett. **23**(19), 1370–1372 (2011).
15. L. Fu, Q. Li, P. Kuffner, G. Jolley, P. Gareso, H. H. Tan, and C. Jagadish, "Two-color InGaAs/GaAs quantum dot infrared photodetectors by selective area interdiffusion," Appl. Phys. Lett. **93**(1), 013504 (2008).
16. MaxCap-OM3 - 10 Gb/s multimode optical fiber, high-speed laser-launch multimode fiber (OM3), http://communications.draka.com/sites/usa/Pages/MultiModeFibers_MaxCap.aspx (2013).
17. A. Aguayo, "Advances in high frequency printed circuit board materials," Microwave Eng. Europe, December 2009, 11-14 (2009).

1. Introduction

Optical interconnections are utilized to meet the increased level of demand pertaining to internet data traffic and to overcome the limitations of electrical interconnects due to advantages such as a short signal delay, a light weight, lower power consumption, and immunity to electromagnetic interference [1–3]. Optical interconnects improve the speed and quality of data transmissions in short-reach applications such as data processing units, optical storage applications and in data centers. The high-storage data processing units of data centers require high-speed data transmission for rack-to-rack, board-to-board and chip-to-chip interconnections, with a design of high-capacity and compact pluggable optical modules for bidirectional optical links. Thus, careful designs of the TRx modules and optical components are desirable to minimize the optical assembly costs while optimizing their performances.

Bidirectional optical links as up- and down-links can be operated in full-duplex or half-duplex mode. During full-duplex mode operation, the optical signals can be transmitted and received simultaneously, while in half-duplex mode, the optical signals can be transmitted or received by time-sharing. Half-duplex bidirectional transmission can be implemented through a single fiber [4] or through two fibers [5]. Full-duplex bidirectional transmission has been implemented through two fibers [1]. In half-duplex optical interconnect applications, the bandwidth of the bidirectional data transmission is reduced, while in full-duplex data transmission, the efficiency is increased by simultaneous data transmission. However, implementation of the full-duplex mode with two fibers increases the number of fibers for bidirectional transmission. An ideal solution to provide rapid data access in a cost-effective structure is full-duplex transmission through a single fiber. However, simultaneous data transmission through a single fiber may cause serious interference between the up- and down-link. Hence, in the proposed bidirectional optical link, we use different wavelengths for the up- and down-link to reduce the optical crosstalk between the up- and down-link through a single fiber.

The design of a bidirectional optical link using a single fiber requires special structures and the integration of a laser diode (LD), a photodiode (PD), and a transceiver (TRx) chip with a surface mirror or a bulk optic mirror [2, 6, 7]. In an early work [6] on a bidirectional module structure using a single fiber, a silicon optical bench (SiOB) with silicon surface mirrors was shown to be capable of surface emitting/receiving LD/PD chips which are monolithically integrated with a TRx chip and mounted on the SiOB. In other work [7] on a bidirectional optical subassembly (OSA) module through a single-mode fiber (SMF), two long wavelengths for the up- and down-link were utilized using a bulk optical mirror in which

#200040 - $15.00 USD Received 23 Oct 2013; revised 7 Dec 2013; accepted 15 Dec 2013; published 17 Jan 2014

a wavelength filter was inserted. However, these bidirectional structures use specialized TRx chips integrated with LD and PD components [2, 6] and complex light-transmission structures with bulky mirrors [6, 7]. Therefore, in this paper, we propose a simplified bidirectional OSA module with the mirror and wavelength filters fabricated into the fiber. In order to reduce the optical crosstalk, two wavelengths of 850 nm and 1060 nm are utilized for the up- and down-link, respectively, which provides wider wavelength separation and thus reduces the interference noise between up- and down-link.

2. Design of the bidirectional OSA module

Several structures of bidirectional optical modules have been reported for full-duplex data transmission through a single fiber [6, 7]. Earlier studies utilized SiOB structures to couple optical transmitter (Tx) and receiver (Rx) chips with a fiber and to place monitoring a PD (M-PD) chip. In these structures, surface mirrors formed on a facet of the SiOB or a bulk mirror were used to deflect beams from a surface-emitting (or to a surface-receiving) chip. In this work, we also utilize a SiOB to place chips and fiber in an OSA module, but mirrors for deflection of beams are formed in the fiber, representing an entirely different structure from those in previous works.

2.1 Structure of the bidirectional OSA module

Figure 1 shows the structure of the bidirectional OSA module designed in this work. It consists of a vertical-cavity surface-emitting laser (VCSEL), surface-receiving PD and M-PD components, a TRx IC board, and a fiber array. In the TRx IC board, multi-channel Tx and Rx IC chips are die-bonded onto a small printed circuit board (PCB) on which impedance-matched metal traces are formed for an electrical connection with the main board of the TRx module. VCSEL, PD and M-PD chips are flip-chip bonded onto individual SiOBs, as shown in Fig. 1. These VCSEL, PD and M-PD SiOBs are attached onto an optical fiber array embedded in a V-groove which is formed in a silicon substrate. In the fabrication of these OSA components, we used standard OM3 multi-mode fibers of which the core diameter is 50 μm. For the active components, we used commercially available Tx/Rx IC chips and VCSEL/PD arrays.

To couple the PD and the fiber, a 45° mirror (mirror-1) is formed at the end of the fiber, similarly to previous works [8, 9]. However, to couple the VCSEL and fiber, another 45° mirror (mirror-2) having a function of a half-mirror is formed in the fiber. For mirror-2, wavelength-filtering layers are deposited on the polished surface of a fiber segment, and this segment is attached to a 45°-polished main fiber. Light with a wavelength of 850 nm is emitted from the VCSEL and reflected at mirror-2, after which it enters the fiber for the up-link. Down-linked light with a wavelength of 1060 nm passes through mirror-2 and is reflected at mirror-1, entering into the PD. To monitor the light intensity from the VCSEL, an optical signal leakage window is formed below the M-PD by scratching the fiber to obtain a small amount of scattered light.

#200040 - $15.00 USD Received 23 Oct 2013; revised 7 Dec 2013; accepted 15 Dec 2013; published 17 Jan 2014

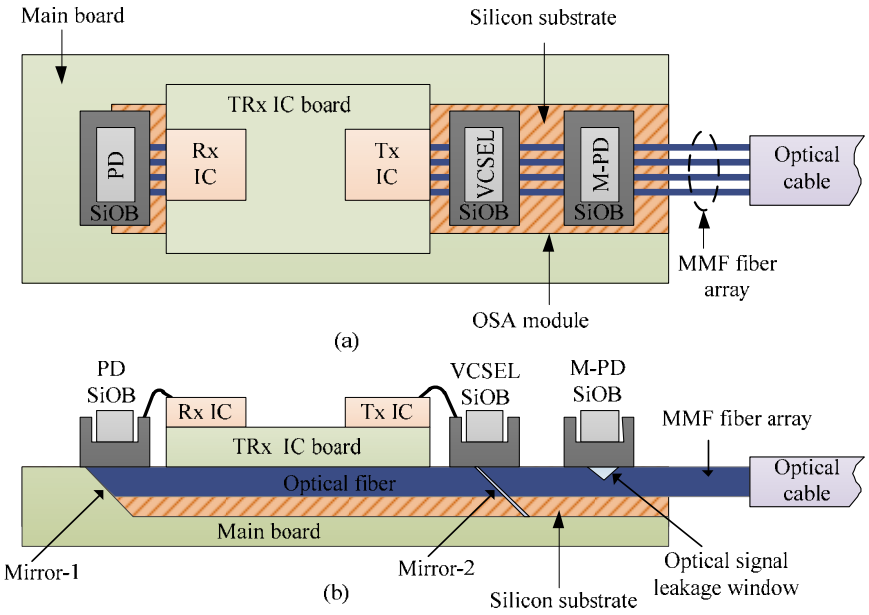

Fig. 1. The structure of the four-channel bidirectional OSA module: (a) top-view and (b) cross-sectional view.

Figure 2 shows the detailed structure of the SiOB onto which the VCSEL, PD, and M-PD array chips are mounted. Each 1x4 array chip is mounted on a separate SiOB. In the SiOB, a square groove is formed to contain the chip and metal lines are formed on the bottom and side wall of the groove for an electrical connection with the chip. In the SiOB, optical via holes are also formed; the walls of the via holes utilize metal deposited layers to facilitate light transmission through the silicon substrate. The space between the bottom of the square groove and the PD/VCSEL chip is left as small as possible to reduce any optical crosstalk that could be induced by the divergence and scattering of light beams. When attaching the SiOB to the silicon substrate, alignment marks are formed with copper plating with a thickness of less 8 μm on the SiOB and the silicon substrate. The thickness of the solder ball is less than 5 μm. Thus, the total distance between the SiOB and the silicon substrate is less than 21 μm. When the fiber is buried in the V-groove formed on the silicon substrate, the distance between the fiber and the SiOB is about 21 μm. In the fabrication of the OSA module, we applied a passive alignment method with these alignment marks. Additionally, the via holes are filled with an index matching oil to reduce scattering at the fiber surface and to maintain the reflection effect of the 45°-mirrors. The diameter of the via holes is 70 μm, which is close to the diameter of the fiber core. The height of the via holes is 125 μm and the pitch of the via holes and the fibers is 250 μm. In order to place the via holes of the SiOB at the exact position above the mirrors or at the leakage windows of the fiber array, alignment marks are made on the silicon substrate and on the bottom side of the SiOB substrate.

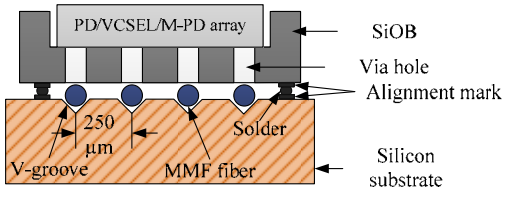

Fig. 2. Detailed structure of the SiOB used to package the VCSEL, PD, and M-PD array chips on the fiber array.

#200040 - $15.00 USD Received 23 Oct 2013; revised 7 Dec 2013; accepted 15 Dec 2013; published 17 Jan 2014

For an efficient alignment of the fibers and the SiOBs we used the following procedure. Four fibers are placed on the V-grooved Si substrate and mounted using an epoxy. This mounted block with the fibers and the Si substrate is polished to make 45° surfaces on both sides. The 45° surfaces are mechanically polished with a deviation of ± 1° using a minute jig and a commercialized polishing machine [8]. Wavelength-filtering layers are deposited on the polished surfaces of the block. The main fibers to couple to mirror-2 of this block are similarly polished mounting on another V-grooved Si substrate and attached to the block using an index-matching epoxy. The SiOBs are placed on the Si substrate using align marks made on the Si substrates and the SiOBs. In a ray trace simulation for the geometries of the 850 nm devices and SiOBs, the alignment tolerance to attain a total coupling loss within 3 dB on both the VCSEL and PD sides is about ± 10 μm in the lateral and longitudinal (along the fiber) directions from the central position of the mirrors. From our alignment procedure, the SiOBs could be placed within ± 3 μm misalignment in the lateral direction and within ± 5 μm in the longitudinal direction, which is expected to be in the range of the 3 dB tolerance for the 850 nm devices. In the rotational angle along the fiber axis, the 45° mirrors can be quite precisely located since the fiber array is already mounted on the Si substrate block and formed the mirrors together.

2.2 Signal transmission in the bidirectional OSA module

The light transmission and receiving schemes of the OSA module are shown in Fig. 3(a). For light transmission (up-link), a wavelength of 850 nm (λ_1) is used, and for light receiving (down-link), a wavelength of 1060 nm (λ_2) is used. Two mirrors, mirror-1 and mirror-2, are located in the optical fiber array to transmit and receive the λ_1 and λ_2 optical signals, respectively. In order to transmit the optical signal of wavelength, λ_1, which is emitted from the VCSEL array, optical signals are sent through the via hole and then reflected into the embedded fiber array by mirror-2. Because mirror-2 has wavelength-filtering layers, the incoming optical signal of wavelength λ_2 passes mirror-2 and is then reflected at mirror-1 to the PD through the via hole of the PD-SiOB. For the M-PD, the scattered light at the leakage window is also guided through the via hole of the SiOB. A photograph of the OSA module is shown in Fig. 3(b), showing the three separate SiOBs for the PD, the VCSEL and the M-PD array chips.

For the leakage window under the M-PD, a scratch is formed only on the clad layer of the fiber to scatter the evanescent light wave. Evanescent waves for sensing and monitoring optical signals from the surfaces of optical waveguides are widely used in optical interconnection [10] and optical sensor applications [11]. The working principle of our optical leakage window is based on that of a structure introduced earlier [10], due to the effectiveness of its evanescent wave for monitoring with a small amount of loss of the transmitting light. In our structure, the leakage window was designed to scatter 5% (~0.2 dB) of the intensity of the transmitted light, which does not cause a significant loss in the optical link and which also provides enough light to the M-PD. To scatter this amount of light, the depth of the scratch was estimated to be near 35 μm from the surface of the fiber by the measurement using a power meter. The scattered power was so sensitively varied near this depth that the detected powers showed considerable fluctuation from sample to sample. Thus, we controlled the scratching process to attain a detected power from each scratch within 2 dB of the transmitted power. On the other hand, the evanescent field can be influenced by the variation of the modes in the fiber core, which could occur during the change of the intensity of the VCSEL source. However, the M-PD has a fairly low bandwidth compared to the modulation bandwidth of the light signal, and thus the time-averaged field should be less sensitive to the variation of the modes during high-speed modulation. In our experiment, the optical power detected from the M-PD was stably maintained during VCSEL modulation.

#200040 - $15.00 USD Received 23 Oct 2013; revised 7 Dec 2013; accepted 15 Dec 2013; published 17 Jan 2014

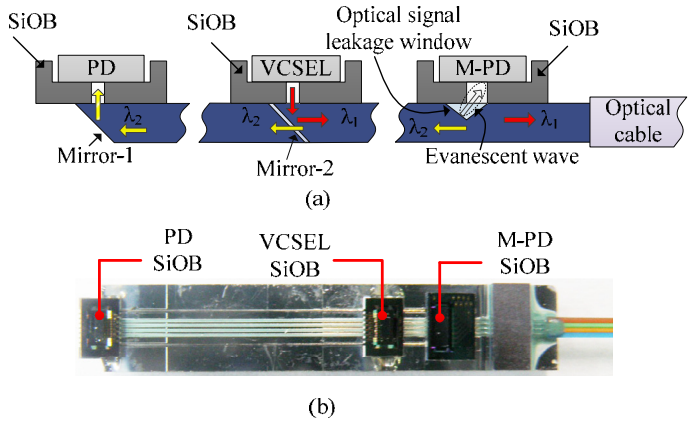

Fig. 3. The bidirectional OSA module: (a) light receiving and transmission schemes for the bidirectional optical link and (b) a photograph of the assembled OSA module.

3. Implementation of the OSA module and components

The stability, the coupling loss and the crosstalk noise of the four-channel OSA module were measured for error-free and successful data transmission in the bidirectional optical link. Thermal shock tests were also done to evaluate the reliability of the device and to assess the parasitic heating effects with temperature changes. The optical crosstalk between the channels of the OSA module was measured to verify the presence of inter-channel isolation. Further, the coupling losses from the VCSEL to the fiber and from the fiber to the PD were measured to estimate the available power budget and power margin for the transmission of optical signals up to 100 m.

3.1 Wavelength separation of the bidirectional link and crosstalk

In the design of our TRx module, two wavelengths of 850 nm and 1060 nm are utilized to reduce the optical crosstalk between the up- and down-link for error-free data transmission. Meanwhile, VCSELs for optical interconnect applications which work with wavelengths of 850 nm and 980 nm are well developed and effectively being utilized in optical interconnect applications, operating at high data rates [12, 13]. Hence, utilizing these two wavelengths of 850 nm and 980 nm can help to isolate the signals between the up- and down-link. However, the responsivities of the PDs to detect these wavelengths could overlap, as shown in Fig. 4. Figure 4 shows the responsivities of commercially available PDs for $In_{0.5}Ga_{0.5}P/GaAs$ and $In_{0.5}Ga_{0.5}As/GaAs$ PIN PDs, as used in this work to detect the 850 nm and 1060 wavelengths, respectively. The responsivity of an $In_{0.53}Ga_{0.47}As/In_{0.52}Al_{0.48}As$ PIN PD for 980 nm is also compared. Each responsivity curve is normalized to its own maximum. As shown in Fig. 4, the responsivity of PIN PDs is usually wider than the wavelength of interest, which may also vary with the temperature [14, 15]. This can lead to crosstalk and signal reliability issues. Thus, in the proposed bidirectional OSA module design, we choose the two wavelengths of 850 nm and 1060 nm, as these wavelengths show less overlap in the responsivity curves of the corresponding PDs. Hence, using two wavelengths with wider separation reduces the optical crosstalk between the transmitted and the received optical signals.

#200040 - $15.00 USD Received 23 Oct 2013; revised 7 Dec 2013; accepted 15 Dec 2013; published 17 Jan 2014

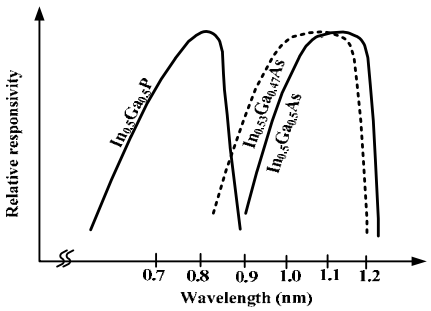

Fig. 4. The relative responsivities of PDs for different wavelengths.

In order to accomplish bidirectional transmission using wavelengths of 850 nm and 1060 nm, two kinds of wavelength-filtering mirrors are required. For the up-link module sending signals from an 850 nm VCSEL, the wavelength-filtering mirror (mirror-2) requires reflection of the 850 nm wavelength and transmission of the 1060 nm wavelength. For the down-link module sending signals from a 1060 nm VCSEL, the mirror requires reflection of the 1060 nm wavelength and transmission of the 850 nm wavelength. A detailed description of this wavelength management scheme for data transmission will be given later in Fig. 9. The wavelength-filtering mirrors were prepared by the deposition of 20 periods of Ti_3O_5/SiO_2 layers on the 45°-polished silica fiber. For filtering the 850 nm wavelength, Ti_3O_5 layer was deposited first, and for filtering the 1060 nm wavelength, SiO_2 layer was deposited first on the silica surface. Figure 5 shows the simulation data of the transmittances for the two kinds of wavelength-filtering mirrors. The simulation result shows the reversed transmittances for the 850 nm and 1060 wavelengths for the two mirrors. The transmittance and reflectance were also identified experimentally in the four-channel modules, as presented in Fig. 6. The measured transmittance of light is about 85 ~88% for the 850 nm wavelength and the reflectance is about ~95% for the 1060 nm wavelength in the up-link module, as shown in Fig. 6(a). While, in the down-link module the transmittance is about 86 ~89% for 1060 nm and the reflectance is about ~95% for 850 nm, as seen in Fig. 6(b).

Note here that for mirror-1 at the end of the fiber, we also deposited wavelength-filtering layers, reversing the filtering wavelengths relative to the layers for mirror-2. Specifically, 850 nm filtering layers are deposited on mirror-1 for the up-link module and 1060 nm filtering layers for the down-link module. Those depositions exhaustively remove the optical crosstalk on the receiver sides. Hence, the crosstalk between the up- and down-link can be minimized. Note also that if the fiber segments are prepared by coating the 850 nm and 1060 nm filtering layers on each 45° end of the segments, they can be used for both the up- and down-link modules, just selecting one end corresponding to mirror-2 and attaching to the main transmission fiber. Thus, the coating on mirror-1 does not incur an additional cost in the processes of preparing the two kinds of mirrors.

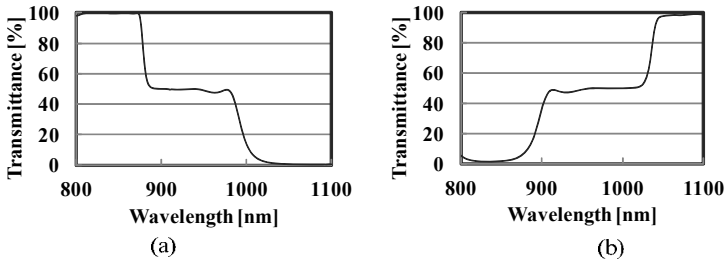

Fig. 5. Simulated transmittance vs wavelength curves for the wavelength-filtering mirrors used in the OSA modules (a) for the up-link and (b) for the down-link.

#200040 - $15.00 USD Received 23 Oct 2013; revised 7 Dec 2013; accepted 15 Dec 2013; published 17 Jan 2014

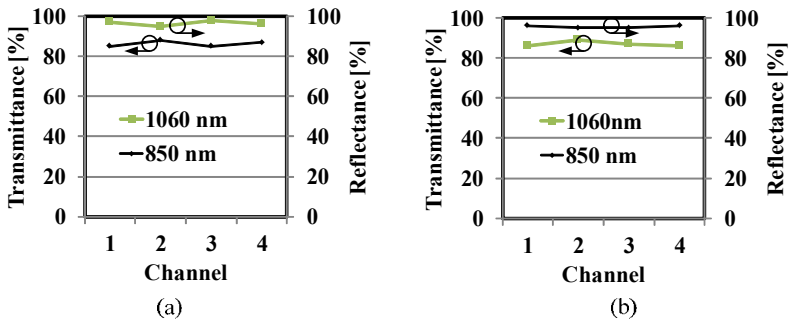

Fig. 6. Measured transmittances and reflectances of the wavelength-filtering mirrors (a) for the up-link and (b) for the down-link.

Figure 7 shows the measured optical crosstalk of each channel with and without the M-PD component. The typical optical crosstalk between the channels is about −45 dB. A higher crosstalk value is obtained for the OSA module with M-PD. This can be attributed to the higher loss due to the presence of the M-PD at the leakage window.

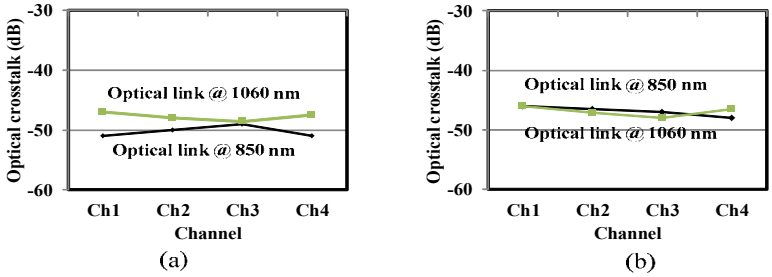

Fig. 7. The measured optical crosstalk of the bidirectional optical link (a) without the M-PD and (b) with the M-PD components.

3.2 Reliability tests of optical components

The results of the reliability test for the VCSEL and PD are shown in Fig. 8. The reliability tests of the VCSEL light power and the responsivity of the PD for the two wavelengths of 850 nm and 1060 nm were assessed during thermal variation of 50 cycles in a range of 0 þC ~70 þC, following the Telcordia reliability assurance requirements (GR-468). After the thermal variation, the change of the VCSEL threshold current, I_{th}, was less than 0.8 mA. Before the thermal variation, the average output light power of the VCSEL arrays were 2 mW and 0.7 mW at wavelengths of 850 nm and 1060 nm, respectively, and the average responsivities of PD arrays were 0.35 A/W and 0.65 A/W at wavelengths of 850 nm and 1060 nm, respectively. After thermal variation, the change in these VCSEL output light power and PD responsivities are less than 10% changes, as shown in Figs. 8(a)-(d). However, these results indicate that the change of the VCSEL output light power is slightly more severe than the change of the PD responsivity due to the inherent thermal sensitivity of the VCSEL light power [12, 13].

#200040 - $15.00 USD Received 23 Oct 2013; revised 7 Dec 2013; accepted 15 Dec 2013; published 17 Jan 2014

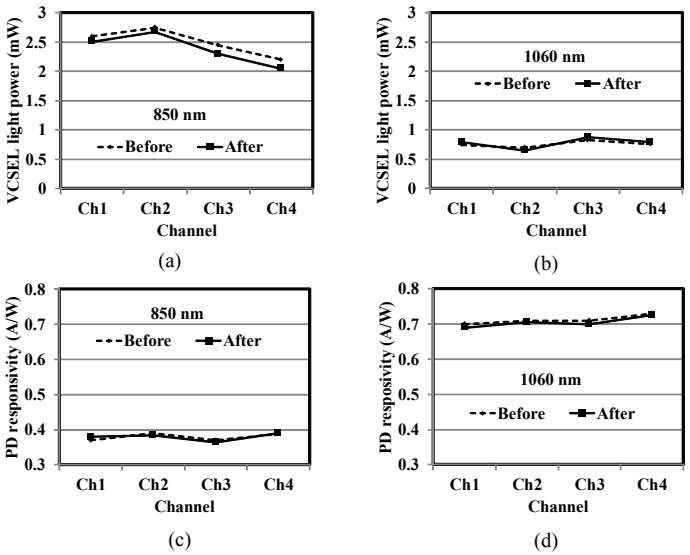

Fig. 8. Results of the reliability test during the thermal variation assessment. The VCSEL light power and PD responsivities are compared before and after thermal variation: (a) light power at 850 nm, (b) light power at 1060 nm, (c) responsivity at 850 nm, and (d) responsivity at 1060 nm.

3.3 Optical link loss measurement

In order to analyze the end-to-end optical signal transmission, the coupling losses from the VCSEL to the PD light path were measured using the measurement setup shown in Fig. 9. The coupling loss measurement is done both with and without M-PD to ascertain that the optical losses are within the available power budget.

The measured coupling losses with and without M-PD shown in Table 1 are taken as the average of all four-channels. The optical coupling loss from the VCSEL to the fiber at a wavelength of 1060 nm is higher than the coupling loss at 850 nm. This result may be due to the higher full-width divergence angle of 33þ in the 1060 nm VCSEL compared to that divergence angle of 19þ in the 850 nm VCSEL. The aperture sizes of the PDs are 60 μm and 50 μm for wavelengths of 850 nm and 1060 nm, respectively, having only a small difference. Thus, it could explain the result of that the coupling losses from the fiber to PD show relatively small differences at 850 nm and 1060 nm.

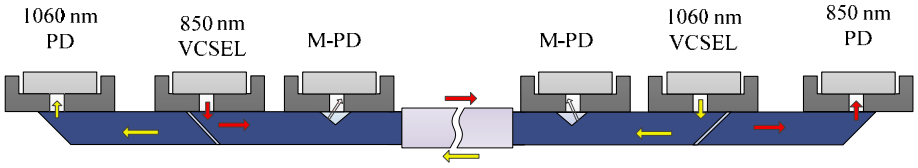

Fig. 9. Light transmission scheme of an end-to-end optical link using the proposed bidirectional OSA modules.

#200040 - $15.00 USD Received 23 Oct 2013; revised 7 Dec 2013; accepted 15 Dec 2013; published 17 Jan 2014

Table 1. End-to-end Optical Coupling Loss of the OSA-based Bidirectional Optical Link

Coupled device and wavelength		Optical coupling loss (dB)		Total coupling loss (dB)
		VCSEL → Fiber	Fiber → PD	
VCSEL without M-PD	@850 nm	0.6	0.8	1.4
	@1060 nm	2.4	0.7	3.1
VCSEL with M-PD	@850 nm	1.4	2.7	4.1
	@1060 nm	3	1.8	4.8

The measurement results of the total coupling loss for end-to-end coupling in the bidirectional optical link with and without M-PDs are shown in Figs. 10(a) and 10(b), respectively. The total coupling loss with M-PD including the coupling losses from the VCSEL to the fiber and from the fiber to the PD is slightly higher than that in the case without the M-PD component. This may be due to the loss of the optical signal caused by the leakage windows which are formed in the samples coupled with the M-PD, as revealed in Table 1. The increment of the loss (in the average value of the four channels) attributed to the leakage window for each coupling is dispersed in the range of 0.6 ~1.9, which is higher than our target value (0.2 dB) established in the design of the leakage window. Thus, to reduce this loss, careful control of V-scratch may be required in the sawing process to form the leakage window. Nevertheless, the total coupling losses from the VCSEL to the PD are less than 5 dB for both the 850 nm and 1060 nm optical links with and without the M-PD component, which indicates that the available power budget of the optical link should be higher than this value.

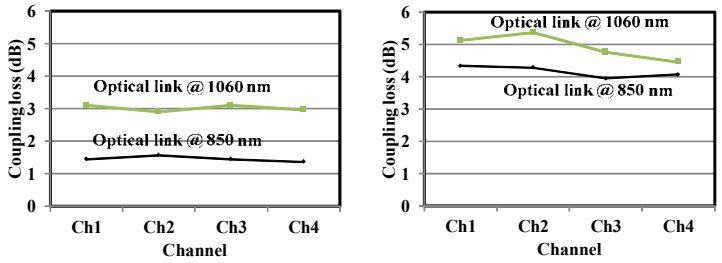

Fig. 10. The measured coupling loss of the bidirectional end-to-end optical link: (a) without M-PD and (b) with M-PD components.

3.4 Power budget of the optical link

The measurements of the coupling losses discussed in the previous section are used to estimate the available power budget and power margin for the transmission of optical signals within 100 m. Table 2 shows a summary of the specifications (measured and recommended values) for the estimation of the end-to-end optical link power budget and power margin at a data rate of 10 Gb/s using a multi-mode fiber (MMF) array with a core size of 50 μm. The sensitivity of the Rx module is estimated using an Rx input sensitivity of 20 μA and the minimum PD responsivity from the measured results shown in Figs. 8(b) and 8(d). The measured minimum PD responsivity is 0.35 A/W and 0.65 A/W at wavelengths of 850 nm and 1060 nm, respectively. The estimated input sensitivity levels of the Rx modules are −12.4

#200040 - $15.00 USD Received 23 Oct 2013; revised 7 Dec 2013; accepted 15 Dec 2013; published 17 Jan 2014

dBm and −15.1 dBm at wavelengths of 850 nm and 1060 nm, respectively. Similarly, the available output power of the Tx modules is estimated from the measured results of the VCSEL light power shown in Figs. 8(a) and 8(c). The available VCSEL light power levels are equal to 2 dBm and −1.5 dBm at wavelengths of 850 nm and 1060 nm, respectively.

Table 2. Specifications for the End-to-end Optical Link Power Budget Estimation

Category	Item	@850 nm	@1060 nm
Measured	Tx power (P_{Tx}), dBm	2	−1.5
Measured	Coupling loss (P_{CL}), dB	4.1	4.8
Measured	Rx sensitivity (P_{Rx}), dBm	−12.4	−15.1
Recommended	Margin (P_m), dB	2	2
Recommended	Distance (L), m	<100	<100
Standard	Fiber loss (P_F), dB/km	2.2	1.1 *

*Estimated from the data for 1300 nm [16].

Using the data (recommended and/or measured) shown in Table 2, we can estimate the available power budget of the end-to-end optical link. This is obtained by subtracting the minimum receiver input power, P_{Rx}, from the transmitter power, P_{Tx}. The optical power losses in the link between two OSA modules are the summation of the total coupling loss P_{CL} and the optical loss in the fiber P_{FL}. In order to transmit data reliably through an optical link, the available power budget should be greater than the optical link power losses as

$$P_{Tx} - P_{Rx} > P_{CL} + P_{FL}. \tag{1}$$

From Eq. (1), we can also determine the maximum available power margin, P_{MM}, for the bidirectional optical link, as

$$P_{MM} = \left(P_{Tx} - P_{Rx}\right) - \left(P_{CL} + P_{FL}\right). \tag{2}$$

The maximum available power margin, P_{MM}, can be further reduced by considering other impairments, such as inter-channel, inter-mode and inter-symbol types of interference. These forms of interference can also affect the bandwidth of the signal transmission and the transmission distance. Thus, the available power budget of the optical link can be simply estimated from Eq. (1), which involves the subtraction of the Rx sensitivity power, P_{Rx}, from the Tx power, P_{Tx}. These values are approximately 14.4 dB and 13.6 dB for wavelengths of 850 nm and 1060 nm, respectively. In contrast, the optical link power losses are also obtained using Eq. (1) by adding the P_{CL} and P_{FL} losses, estimated as 6.3 dB and 6.9 dB at wavelengths of 850 nm and 1060 nm, respectively. Using Eq. (2), the estimated maximum available power margins are 8.1 dB and 6.7 dB at wavelengths of 850 nm and 1060 nm, respectively. These maximally available power margins are greater than the required power margin of 2 dB, which is required for most optical interconnect systems. Hence, the bidirectional optical link with the proposed OSA modules can be utilized for transmitting data signals within 100 m. However, the achievable distance could be reduced due to various forms of signal impairment.

4. Experimental results

A demonstration system for a four-channel end-to-end bidirectional optical link is shown in Fig. 11. To measure the performance of the fabricated bidirectional OSA modules, four-channel evaluation boards were designed with input and output ports to transmit and receive data signals. Two different modules for the up-link to send 850 nm signals and for the down-link to send 1060 nm signals are installed on the same evaluation boards. These modules were connected using an OM3 standard MMF fibers array with four channels and a length of 2 m to measure the end-to-end optical link. The inset shown in Fig. 11 is a photograph of the main board, including the OSA module with the optical components of the TRx IC board and chips. The main board is connected to an evaluation board for measurement purposes using a 0.8

#200040 - $15.00 USD Received 23 Oct 2013; revised 7 Dec 2013; accepted 15 Dec 2013; published 17 Jan 2014

mm pitch input/output (I/O) connector. The evaluation board is made of a ceramic board filled hydrocarbon material, which has good electrical and thermal properties [17].

4.1 Demonstration of the bidirectional optical link

To demonstrate the bidirectional optical link, frequency responses and eye-diagrams were measured using the evaluation boards shown in Fig. 11. An Anritsu MP1763B pulse pattern generator and an Agilent 86100A oscilloscope are used to feed input electrical signals and to measure output electrical signals to/from the evaluation boards. This setup measures the electrical-to-electrical responses received by the PD and receiver IC after light signal transmission from the VCSEL and driver IC. To measure the responses and eye-diagram separately for each channel, the signal is transmitted through one channel while the other channels are stood as turn-on states without the input of modulated signals. The eye-diagrams were measured using a pseudorandom bit stream of 2^{31}-1. Differential splitter-baluns (5320B-104) were utilized to convert single-ended signals to differential signals for the measurement of the BER and crosstalk. The BER and eye-diagrams were measured at 10 Gb/s/ch to demonstrate the 40 Gb/s bidirectional optical link.

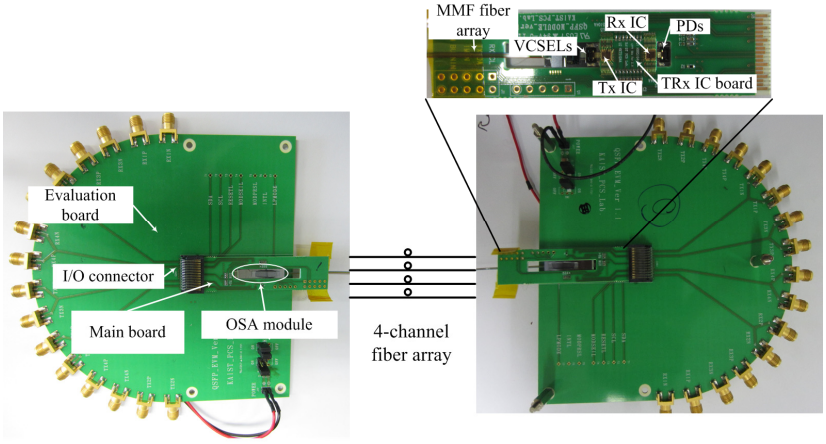

Fig. 11. Photograph of the demonstration system for a four-channel bidirectional optical link with the up-link module (left) and the down link module (right) installed on the same evaluation board: the inset shows a top view of the main board, showing the OSA module with the optical components of the TRx IC board and chips.

Figure 12 shows the measured frequency response of the four-channel optical link and the crosstalk between the channels for a unidirectional up-link. The signal lines are connected to the Tx/Rx ICs, VCSEL/PD and OSA modules on both Tx/Rx sides. Therefore, the measured frequency response includes the influences from these components. All channels have a uniform gain profile with a stable 3-dB bandwidth with a response of about 7.5 GHz, which is enough for 10 Gb/s/ch data transmission. The crosstalk measurement includes the parasitic crosstalk from the bidirectional optical link and the signal lines of the TRx IC board, I/O connectors, and evaluation boards. The average crosstalk from Ch1 to the neighboring channels is less than −25.6 dB; that from Ch2 to the neighboring channels is less than −24.1 dB, that from Ch3 to the other channels is less than −22.6 dB, and that from Ch4 to the other channels is less than −25.2 dB. Hence, the overall crosstalk of the bidirectional optical link from the source to the neighboring channels is less than −22.6 dB. The average crosstalk value was higher than that obtained from a single OSA module, at approximately −45 dB to −50 dB, as the crosstalk measurement was performed with two separate OSA modules attached to the main board and then connected to two evaluation boards. For this reason, crosstalk between the channels occurs due to the electrical and optical signal transmission. However, it is difficult to extract optical crosstalk from electrical crosstalk. Hence, we

#200040 - $15.00 USD Received 23 Oct 2013; revised 7 Dec 2013; accepted 15 Dec 2013; published 17 Jan 2014

measured the crosstalk of the main board (without the OSA module), the I/O connector, and the evaluation board in order to determine the electrical crosstalk between adjacent channels. Average crosstalk ranging from −21 dB to −30 dB was obtained. Thus, the crosstalk contributions of the I/O connector and the evaluation board seriously affect the overall crosstalk measurement of the bidirectional optical link.

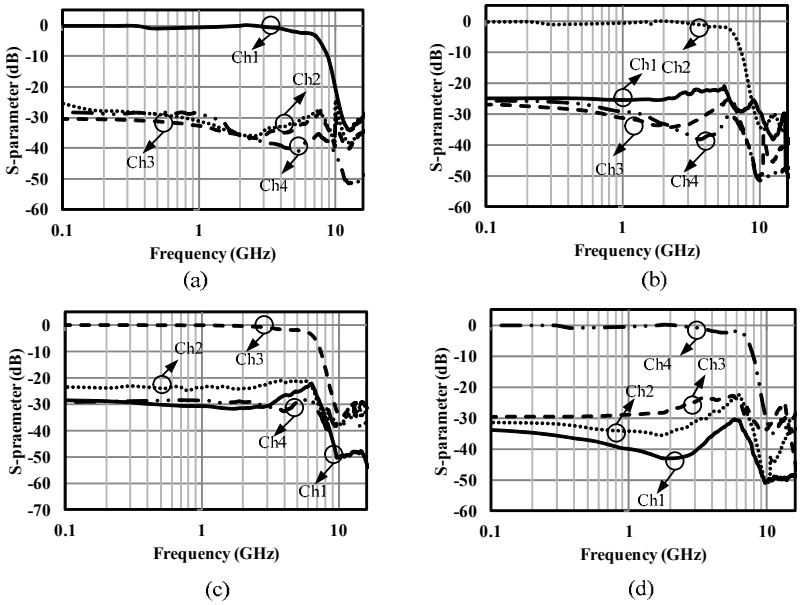

Fig. 12. The measured frequency responses with the crosstalk of the unidirectional up-link: (a) crosstalk from Ch1 to other channels, (b) crosstalk from Ch2 to other channels, (c) crosstalk from Ch3 to other channels and (d) crosstalk from Ch4 to other channels.

Figure 13 shows eye-diagrams of the four-channel half-duplex bidirectional optical link measured at 10 Gb/s/ch. In the half-duplex mode, the up- and down-links are separately operated. For example, for the up-link measurement, the transmitter part in the down-link module is turned-off while the receiver part is turned-on. Each channel shows relatively clear and uniform eyes for both the up- and the down-link. The peak-to-peak jitters for up-link/down-link are less than 28.6/56.0 ps for Ch1, 38.0/41.0 ps for Ch2, 36.8/56.8 ps for Ch3 and 42.7/61.7 ps for Ch4. The measured rise/fall times are less than 31.7/32.5 ps for Ch1, 32.0/30.3 ps for Ch2, 32.9/32.1 for Ch3, and 30.7/27.7 ps for Ch4 for both the up- and the down-link, respectively. The eye-diagram measurement shown in Fig. 13 is the measurement result taken from the optical link including the proposed bidirectional OSA module. In order to measure the eye-diagrams, a pulse pattern generator generates an electrical voltage signal which is then converted to an optical signal by the Tx IC and VCSEL, and using the bidirectional OSA module on the Tx side, the optical signal is transmitted through the optical fiber. The optical signal is then passed to the PD by the OSA module located on the Rx side and finally the photocurrent generated by the PD is converted to an electrical voltage signal with the Rx IC to feed to the oscilloscope. Thus, the eye-diagrams are recorded after converting the optical signal back to the electrical signal by the PD and Rx IC. The eye-diagram is recorded for Ch1 when the signal is transmitted only from Ch1 by the Tx IC and VCSEL on the Tx side and received by the Rx IC and PD on the Rx side. Hence, during the recording of the eye-diagram through Ch1, the other channels (Ch2, Ch3, and Ch4) are not transmitting. Thus, all channels are recorded separately, while the other channels are not transmitting. The down-link with the 1060 nm wavelength has higher jitter compared to the up-link with the 850 nm wavelength. This result may be due to the VCSELs used in the

#200040 - $15.00 USD Received 23 Oct 2013; revised 7 Dec 2013; accepted 15 Dec 2013; published 17 Jan 2014

down-link, which has a wider divergence angle and also higher coupling losses (Fig. 10), and the effects of the conversion of the signal from electrical to optical and optical to electrical.

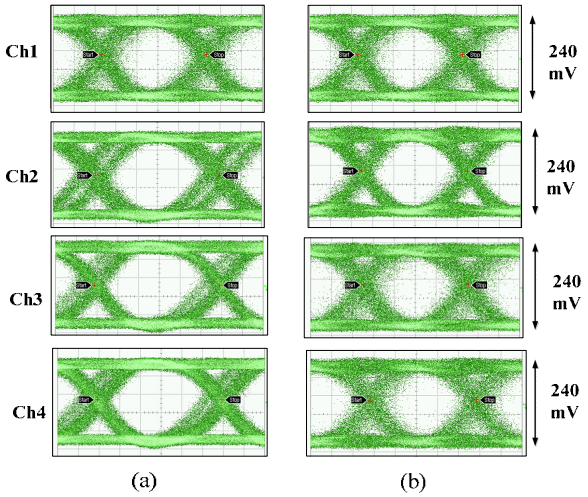

Fig. 13. Measured eye-diagrams of the four-channel half-duplex bidirectional optical link at 10 Gb/s/ch: (a) For the up-link (850 nm) and (b) for the down-link (1060 nm), 16.6 ps/div is shown in the diagram.

Figure 14 shows the measured results of the BER versus the input power at 10 Gb/s/ch with the half-duplex bidirectional optical link for the up- and down-link, separately measured. To measure the BER of the optical link with bidirectional OSA modules, fixed MMF attenuators were utilized. The BER performance levels of the four-channel bidirectional optical link showed uniformity within 1.2 dB. To obtain a BER of less than 10^{-12} for the up- and the down-link, the received light power should be higher than −8 dBm and −6.5 dBm, respectively. The down-link with the 1060 nm wavelength has higher jitter and requires more received power to obtain a BER of less than 10^{-12} compared to the up-link with the 850 nm wavelength, this may be due to the higher end-to-end coupling loss at 1060 nm (Fig. 10).

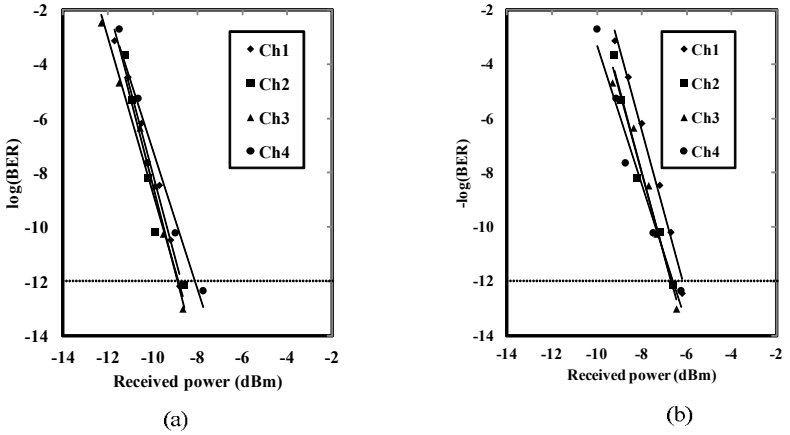

Fig. 14. The BER measurement results of the half-duplex bidirectional optical link at 10 Gb/s/ch: (a) For the up-link (850 nm) and (b) for the down-link (1060 nm).

#200040 - $15.00 USD Received 23 Oct 2013; revised 7 Dec 2013; accepted 15 Dec 2013; published 17 Jan 2014

4.2. Bidirectional optical signal transmission in full-duplex mode

To confirm the full-duplex bidirectional data transmission performance, eye-diagrams and frequency responses were measured and compared to those that occur during the half-duplex mode of operation. For the measurement of the half-duplex mode, the idle transmitter and receiver parts in the up- and down-link modules are turned off, whereas for the full-duplex mode the idle parts are turned on. The eye-diagram openings at 10 Gb/s are clear for both the half-duplex and the full-duplex mode with a peak-to-peak output of 240 mV, as shown in Fig. 15. The eye-diagrams shown in Fig. 15 show that the peak-to-peak jitter increases from 33.6 ps in the half-duplex mode to 35.2 ps in the full-duplex mode. In contrast, the rise/fall times increased from 20.2/26.3 ps in the half-duplex mode to 22.8/29.4 ps in the full-duplex mode. These results indicate that the jitter and rise/fall times of the full-duplex bidirectional operation are slightly degraded compared to those of the half-duplex mode. This degradation might be caused by the inter-mode crosstalk between the up- and down-link originated from the idle electrical and optical components.

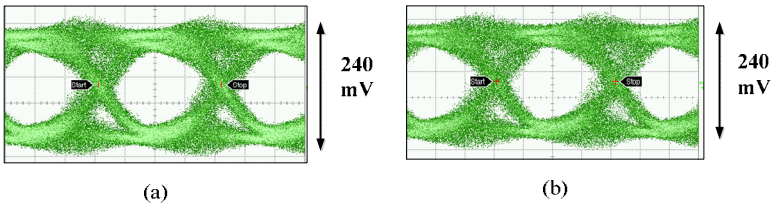

Fig. 15. Measured eye-diagrams of the bidirectional optical link at 10 Gb/s for (a) half-duplex and (b) full-duplex signal transmissions with 24.4 ps/div.

Figure 16 shows the S-parameter measurements of the bidirectional optical link for full-duplex and half-duplex signal transmission. The difference in the 3-dB bandwidth is about 0.1 GHz between these two modes, suggesting that the inter-mode crosstalk is negligible. The frequency response is stable and uniform with a 3-dB bandwidth of 7.5 GHz, which is suitable for 10 Gb/s full-duplex operation. These results indicate that the full-duplex signal transmission undergoes negligible degradation of the bandwidth. From the results shown in Figs. 15 and 16, the slightly higher jitter and bandwidth reduction for full-duplex operation may stem from the small amount of interference between the two widely separated wavelengths of 850 nm and 1060 nm. The crosstalk between the up- and down-link due to the full-duplex operation mode is negligible compared to the inter-channel crosstalk discussed in Fig. 12. Hence, full-duplex operation was successfully demonstrated with the proposed bidirectional OSA module design.

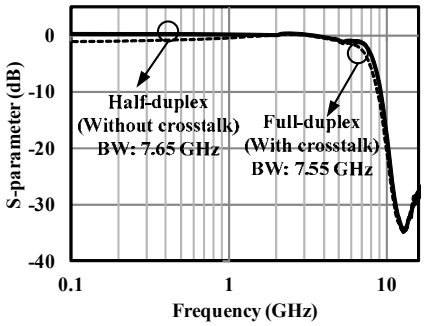

Fig. 16. The measured S-parameters of the bidirectional optical link for full-duplex and half-duplex signal transmission (without and with crosstalk between the up- and down-link, respectively).

#200040 - $15.00 USD Received 23 Oct 2013; revised 7 Dec 2013; accepted 15 Dec 2013; published 17 Jan 2014

5. Conclusion

A 40 Gb/s optical link was demonstrated using a four-channel bidirectional OSA module. The OSA module was designed with individual SiOBs for VCSEL, PD and M-PD array chips; the deflection of light to and from the VCSEL/PD component was realized using 45°-mirrors formed in the fiber, which were then placed under the SiOBs for the VCSEL and the PD. In order to split the up- and down-link light signals with low crosstalk, we selected two wavelengths of 850 nm and 1060 nm, which are widely separated. The up- and down-link light is split with wavelength filters inserted with the mirror under the VCSEL. These structures provide low crosstalk of less than −22.6 dB between neighboring channels in the full-duplex operation mode. The frequency responses for the full-duplex and half-duplex operation modes demonstrated 3-dB bandwidths of 7.55 GHz and 7.65 GHz, respectively, suggesting that the inter-mode crosstalk is negligible. The fabricated bidirectional OSA modules demonstrated successful 40 Gb/s full-duplex optical signal transmission for the up- and down-links, in both cases. The BER measurement was less than 10^{-12} up to 10 Gb/s/ch for each channel at the minimum input power of −8 dBm, which is suitable for data center applications. From the measurement results, the proposed 40 Gb/s OSA module is applicable for high-speed bidirectional data transmission through rack-to-rack and board-to-board optical links with negligible inter-channel and inter-mode crosstalk.

Acknowledgments

This work was supported by the IT R&D program of MKE/KEIT [10039230, Development of a Bidirectional 40 Gbps Optical Link Module with Low Power in the Green Data Center for Smart Working Environment]. It was also supported by the Center for Integrated Smart Sensors funded by the Ministry of Science, ICT & Future Planning as Global Frontier Project (CISS-2012366054191).

#200040 - $15.00 USD Received 23 Oct 2013; revised 7 Dec 2013; accepted 15 Dec 2013; published 17 Jan 2014